Analysis of convergence for initial condition estimation of coupled map lattices based on symbolic dynamics*

Sun Li-Sha(孙丽莎)[a], Kang Xiao-Yun(康晓云)[a]†, and Lin Lan-Xin(林兰馨)[b]

[a] College of Engineering, Shantou University, Shantou 515063, China
[b] Department of Electronic Engineering, City University of Hong Kong, Hong Kong

(Received 31 December 2009; revised manuscript received 2 July 2010)

A novel approach to the inverse problem of diffusively coupled map lattices is systematically investigated by utilizing the symbolic vector dynamics. The relationship between the performance of initial condition estimation and the structural feature of dynamical system is proved theoretically. It is found that any point in a spatiotemporal coupled system is not necessary to converge to its initial value with respect to sufficient backward iteration, which is directly relevant to the coupling strength and local mapping function. When the convergence is met, the error bound in estimating the initial condition is proposed in a noiseless environment, which is determined by the dimension of attractors and metric entropy of the system. Simulation results further confirm the theoretic analysis, and prove that the presented method provides the important theory and experimental results for better analysing and characterizing the spatiotemporal complex behaviours in an actual system.

Keywords: coupled map lattices, convergence, symbolic dynamics, initial condition estimation

PACC: 0545

1. Introduction

Chaotic signals, generated from nonlinear systems, are a class of very important signals, and have a wide application in various engineering contexts such as signal processing, communication and weather forecasting.[1−6] To investigate the characteristics of the spatiotemporal signals, coupled map lattice (CML) is widely used to model practical systems. The CML can reproduce the essential features of spatiotemporal phenomena, in which space–time discretization and continuous state variable are used. Some special high-dimensional chaotic systems are produced by lower-dimensional chaotic units interacting with each other in different coupling ways, such as globally coupled, two-way coupled and one-way coupled manners, i.e. spatiotemporal chaotic systems.[7]

The CML is greatly conducive to the study of the spatiotemporal complex phenomena. Based on the symbolic dynamics techniques, spatiotemporal dynamical behaviours can be further simplified for many purposes. Symbolic vector dynamics, in which the infinite number of finite-length trajectories of the dynamical system is partitioned into a countable number of trajectory-sets in terms of symbolic dynamics,[8] has been an effective tool for understanding and analysing chaotic phenomena. Recently, with the deep research on dynamical characters of the CML systems, the applications cover several aspects of representing quantity of information with symbolic entropy,[9−10] determining pseudo-random properties of chaotic systems[11] and ergodic properties of CML.[12]

Recently, symbolic dynamics has received much attention for estimating the initial condition of CML. In Ref. [13], the algorithm for one-dimensional (1D) chaotic signal estimation was proposed based on the relationship between symbolic sequences and the initial condition of the chaotic system, which was computationally efficient and had the universality. The one-to-one correspondence between the global orbit and the set of admissible codes by taking the Logistic map as a typical example was proved, but no method was given of estimating the initial condition from the spatiotemporal chaotic system. In Ref. [14] was proposed a method which could roughly recover the initial condition from CML without space coupling in terms of statistical properties such as the mean and the variance of the global orbit of CML. The results were further confirmed in Ref. [15] by introducing time-varying parameter into local dynamics in CML. In order to obtain the initial value in each site

*Project supported by the National Natural Science Foundation of China (Grant Nos. 60571066, 60271023 and 61072037), and the Natural Science Foundation of Guangdong Province, China (Grant No. 07008126).
†Corresponding author. E-mail: 08xykang@stu.edu.cn
© 2010 Chinese Physical Society and IOP Publishing Ltd

of CML system, Wang *et al.*[16] presented an algorithm in which the inverse of chaotic map was regarded as being contraction. In Ref. [16] it was demonstrated that any point in the Logistic-CML system could converge to its initial condition with respect to sufficient backward iterations. In Refs. [17] and [18], the conclusion in Ref. [16] was extended to the cases of Skews-tent-CML, Piece-linear-CML and Chebyshev-CML. In Ref. [19], the precondition in Ref. [16] was proved not to hold true. In addition, any point in state space was not necessary to converge to its initial condition, which is directly relevant to the coupling coefficient and local mapping function.

Notice that the bound condition was assumed to be open in Refs. [16]–[19]. However, we are not sure of the bound condition in an actual system, which is definitely much more complex than this hypothesis and has a broad variety of forms existing. Therefore, this assumption is replaced with another form to study whether the conclusion in Ref. [19] still holds. Meanwhile, the error bound for estimating initial condition in CML is proposed, which is relevant to the dimension of attractors and metric entropy of CML. Moreover, the bound gradually weakens exponentially. Simulations show that error of the estimator in each backward iteration process is reliably less than the error bound.

The rest of the present paper is organized as follows. In Section 2, a computationally efficient algorithm with symbolic dynamics is developed for estimating initial condition of spatiotemporal complex system. In Section 3, both convergence and divergence in backward iteration process are analysed for different CMLs. In Section 4, the error bound for effectively estimating initial condition is proposed. In Section 5, the performance is estimated and investigated. Finally, the conclusions drawn from the present approach are given in Section 6.

2. Inverse problem

The typical diffusive CML model is described as

$$x_{n+1}^i = (1-\varepsilon)f(x_n^i) + \frac{\varepsilon}{2}[f(x_n^{i+1}) + f(x_n^{i-1})], \quad (1)$$

where x_n^i denotes the observable state, in which n represents the time step and i ($i = 1, 2, \ldots, L$ = system size) with periodic boundary conditions is the spatial site, i.e.,

$$x_n^{i+L} = x_n^i. \quad (2)$$

The local dynamics function $f : I \to I$ is a unimodal map, where I represents the phase space. ε indicates the coupling strength.

Let $P = \{P_0, P_1, \ldots, P_{m-1}\}$ be a finite disjoint partition of a phase space I, i.e., $\bigcap_{j=0}^{m-1} P_j = \varphi$, and $\bigcup_{j=0}^{m-1} P_j = I$, the time series $S = \{0, 1, \ldots, m-1\}$ is defined as a symbol set of the given system. Consequently, if x_n^i at time n of the system trajectory is in the jth element of the partition, a symbol $s_n^i = j, j \in S$ can be assigned based on the following some partition rules. Then Eq. (1) produces the symbolic vector $\boldsymbol{s}_n = [s_n^1, s_n^2, \ldots, s_n^L]^{\mathrm{T}}$ at nth iteration and the symbolic vector sequences $\{\boldsymbol{s}_0, \boldsymbol{s}_1, \ldots, \boldsymbol{s}_n, \ldots\}$ from 0th iteration, which describes the orbits of the global complex system at different times. Let $\boldsymbol{x}_n = [x_n^1, x_n^2, \ldots, x_n^L]^{\mathrm{T}}$, and $\boldsymbol{f}(\mathrm{x}_n) = [f(x_n^1), f(x_n^2), \ldots, f(x_n^L)]^{\mathrm{T}}$, then Eq. (1) can be concisely described as $\boldsymbol{x}_{n+1} = \boldsymbol{A} \times \boldsymbol{f}(\boldsymbol{x}_n)$, where $\boldsymbol{A}$ is an $L \times L$ coupling matrix given as

$$\boldsymbol{A} = \begin{bmatrix} 1-\varepsilon & \varepsilon/2 & 0 & \ldots & 0 & \varepsilon/2 \\ \varepsilon/2 & 1-\varepsilon & \varepsilon/2 & \ldots & 0 & 0 \\ 0 & \varepsilon/2 & 1-\varepsilon & \ldots & 0 & 0 \\ \vdots & \ddots & \ddots & \ddots & \vdots & \vdots \\ 0 & 0 & 0 & \varepsilon/2 & 1-\varepsilon & \varepsilon/2 \\ \varepsilon/2 & 0 & 0 & \ldots & \varepsilon/2 & 1-\varepsilon \end{bmatrix}_{L\times L}. \quad (3)$$

When $\boldsymbol{A}$ is nonsingular, then $\boldsymbol{f}(\boldsymbol{x}_n) = \boldsymbol{A}^{-1}\boldsymbol{x}_{n+1}$. Because f is a monotonic function in each interval respectively while symbol s_n^i is known, we have

$$\begin{aligned} \boldsymbol{x}_n &= \boldsymbol{f}_{s_n}^{-1}(\boldsymbol{A}^{-1}\boldsymbol{x}_{n+1}) \\ &= \boldsymbol{f}_{s_n}^{-1} \circ \boldsymbol{A}^{-1}(\boldsymbol{x}_{n+1}) \\ &= \boldsymbol{H}_{s_n}^{-1}(\boldsymbol{x}_{n+1}), \end{aligned} \quad (4)$$

where $\boldsymbol{H}_{s_n}^{-1} = \boldsymbol{f}_{s_n}^{-1} \circ \boldsymbol{A}^{-1}$: $I^L \to I^L$. In this paper, both Logistic map $f_L(x) = 4x(1-x)(x \in [0,1])$ and tent map $f_{\mathrm{T}}(x) = 1 - 2|x - 0.5|\,(x \in [0,1])$ as local mapping functions in CML are mainly discussed. $\boldsymbol{H}_{\mathrm{Ls}_n}^{-1}$ and $\boldsymbol{H}_{T\boldsymbol{s}_n}^{-1}$ denote the inverse maps of Logistic-CML and Tent-CML respectively.

First of all, we introduce the definitions of contraction maps and the concepts of the whole convergence (WC) and the whole divergence (WD) in order to understand the convergence and divergence (CD) in backward iteration of CML.

Lemma (i.e., contraction mapping theorem):

Let $T : X \to X$ such that $d(Tx, Ty) \le \gamma d(x, y)$, where $0 < \gamma < 1$ for all x, y in a complete metric space (X, d), then there will be a fixed point $\bar{x}$ in X for T. Thus, for any initial value $x_0 \in X$, $\lim_{n\to\infty} T^n x_0 = \bar{x}$.

The γ_n in $d(Tx_n, Ty_n) = \gamma_n d(x_n, y_n)$ is defined as a convergent or divergent factor. When $0 < \gamma_n < 1$, γ_n is regarded as a convergent factor, and T is taken to be convergent at the nth iteration. Otherwise, γ_n is called a divergent factor, while T is divergent at nth iteration. Therefore, if $0 < \gamma_n < 1$ exists for any n, T is thought as a contraction map. Letting $E = \{e_1, e_2, \ldots, e_I\}$ and $G = \{g_1, g_2, \ldots, g_J\}$, where $n \in G$ and $\gamma_n \geq 1$, we know that T is convergent in some subsets of phase space X and divergent in other subsets. As the convergent strength is much higher than the divergent strength, T is WC. Otherwise, T becomes WD. Only if the inverse of CML is a contraction map or WC, can the initial conditions of the complex system be recovered according to the proposed algorithm.

3. CD

In this section, we discuss the CD of $\boldsymbol{H}_{\boldsymbol{s}_n}^{-1}$, which is determined by both $\boldsymbol{f}_{\boldsymbol{s}_n}^{-1}$ and $\boldsymbol{A}^{-1}$. The CD of $\boldsymbol{f}_{\boldsymbol{s}_n}^{-1}$ has been investigated in detail in Ref. [19] and was found that the inverse map of unimodal chaotic Logistic map is WC, whereas Tent map is globally contracting. Therefore, we need to investigate only the CDs of $\boldsymbol{A}^{-1}$ and $\boldsymbol{H}_{\boldsymbol{s}_n}^{-1}$.

3.1. CD of inverse matrix $\boldsymbol{A}^{-1}$

For any $\boldsymbol{x}_n, \boldsymbol{y}_n \in I^L$, where $\boldsymbol{x}_n = [x_n^1, x_n^2, \ldots, x_n^L]^{\mathrm{T}}, \boldsymbol{y}_n = [y_n^1, y_n^2, \ldots, y_n^L]^{\mathrm{T}}$, define

$$d(\boldsymbol{x}, \boldsymbol{y}) = \|\boldsymbol{x}_n - \boldsymbol{y}_n\| = \max_{1 \leq i \leq L} \left| x_n^i - y_n^i \right|. \quad (5)$$

When $|\boldsymbol{A}| \neq 0$, define $\boldsymbol{A}^{-1} = (a_{ij})_{L \times L}$, and $\left\|\boldsymbol{A}^{-1}\right\| = \max\limits_{1 \leq i \leq L} (\sum_{j=1}^{L} |a_{ij}|)$. Meanwhile, let $\boldsymbol{x}'_n = \boldsymbol{A}^{-1}\boldsymbol{x}_n = [\alpha_n^1, \alpha_n^2, \ldots, \alpha_n^L]^{\mathrm{T}}$, $\boldsymbol{y}'_n = \boldsymbol{A}^{-1}\boldsymbol{y}_n = [\beta_n^1, \beta_n^2, \ldots, \beta_n^L]^{\mathrm{T}}$, then

$$\begin{aligned} d(\boldsymbol{x}'_n, \boldsymbol{y}'_n) &= \left\|\boldsymbol{A}^{-1}\boldsymbol{x}_n - \boldsymbol{A}^{-1}\boldsymbol{y}_n\right\| \\ &= \max_{1 \leq i \leq L} \left| \sum_{j=1}^{L} a_{ij}(x_n^j - y_n^j) \right| \\ &\leq \left(\max_{1 \leq i \leq L} \sum_{j=1}^{L} |a_{ij}| \right) \cdot \max_{1 \leq j \leq L} \left| x_n^j - y_n^j \right| \\ &= \left\|\boldsymbol{A}^{-1}\right\| d(\boldsymbol{x}_n, \boldsymbol{y}_n). \end{aligned} \quad (6)$$

Because $\|\boldsymbol{A}\| = 1$, the distance of two points in phase space, I^L, can also be expressed as

$$\begin{aligned} & d(\boldsymbol{x}_n, \boldsymbol{y}_n) \\ &= d(\boldsymbol{A}\boldsymbol{x}'_n, \boldsymbol{A}\boldsymbol{y}'_n) \\ &= \|\boldsymbol{A}\boldsymbol{x}'_n - \boldsymbol{A}\boldsymbol{y}'_n\| \\ &\leq \|\boldsymbol{A}\| \, \|\boldsymbol{x}'_n - \boldsymbol{y}'_n\| \\ &= d(\boldsymbol{x}'_n, \boldsymbol{y}'_n), \\ &\text{i.e.,} \quad d(\boldsymbol{A}^{-1}\boldsymbol{x}_n, \boldsymbol{A}^{-1}\boldsymbol{y}_n) \geq d(\boldsymbol{x}_n, \boldsymbol{y}_n). \end{aligned} \quad (7)$$

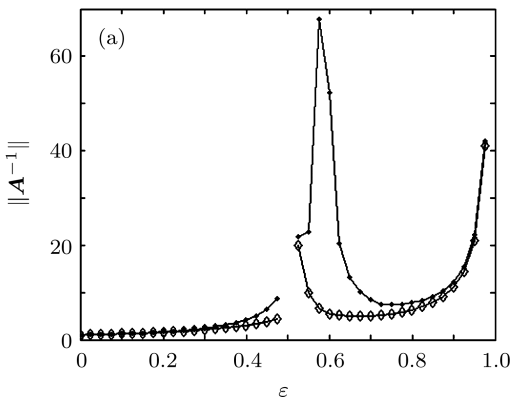
From inequalities (6) and (7), we obtain

$$d(\boldsymbol{x}_n, \boldsymbol{y}_n) \leq d(\boldsymbol{x}'_n, \boldsymbol{y}'_n) \leq \left\|\boldsymbol{A}^{-1}\right\| d(\boldsymbol{x}_n, \boldsymbol{y}_n). \quad (8)$$

Due to $\left\|\boldsymbol{A}\boldsymbol{A}^{-1}\right\| = 1$, then

$$\begin{aligned} & 1 = \left\|\boldsymbol{A}\boldsymbol{A}^{-1}\right\| \leq \|\boldsymbol{A}\| \left\|\boldsymbol{A}^{-1}\right\| \leq \left\|\boldsymbol{A}^{-1}\right\|, \\ & \text{i.e.,} \quad \left\|\boldsymbol{A}^{-1}\right\| \geq 1. \end{aligned} \quad (9)$$

According to the contraction mapping theorem, from inequalities (8) and (9), it follows that $\boldsymbol{A}^{-1}$ is not a contraction map, but a divergent map. Figure 1 shows the values of $\left\|\boldsymbol{A}^{-1}\right\|$ at different values of coupling coefficient ε and the system size L. Figure 1 gives the relationships between $\left\|\boldsymbol{A}^{-1}\right\|$ and coupling coefficient under different numbers of site L. We can see from Fig. 1(a) that $\left\|\boldsymbol{A}^{-1}\right\|$ slowly increases as the coupling coefficient increases when $\varepsilon < 0.5$. For $\varepsilon < 0.5$, $\left\|\boldsymbol{A}^{-1}\right\|$ changes fast with ε, and is affected by the number of sites in CML. In addition, when $\varepsilon \in [0.4, 0.5)$, the value of $\left\|\boldsymbol{A}^{-1}\right\|$ also has a relation with the number of sites L. Figure 1(b) clearly shows the relationship between L and $\left\|A^{-1}\right\|$ for small values of coupling coefficient, such as $\varepsilon \in [0, 0.3]$. The results in Fig. 1 indicate that when $L < 10$, $\left\|\boldsymbol{A}^{-1}\right\|$ is related with L. When the number of sites increases, $\left\|\boldsymbol{A}^{-1}\right\|$ is not affected by L. Meanwhile, it can be found that $\left\|\boldsymbol{A}^{-1}\right\| \geq 1$ as given in Eq. (9).



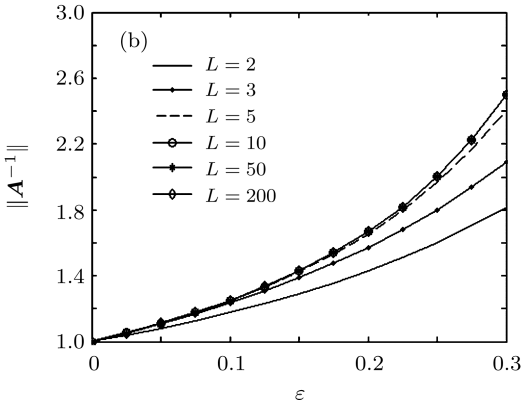


Fig. 1. Relationships between $\|\boldsymbol{A}^{-1}\|$ and the coupling coefficient under different values of L, with (a) ε evaluated in a range of 0–1 ($\varepsilon \in [0,1]$) as A is nonsingular and (b) 0–0.3 ($\varepsilon \in [0,0.3]$).

3.2. Analysis of CD of $\boldsymbol{H}^{-1}_{\boldsymbol{s}_n}$

3.2.1. CD of $\boldsymbol{H}^{-1}_{\mathrm{L}\boldsymbol{s}_n}$

A unimodal chaotic Logistic map can be defined as $f_L(x_n) = 4x_n(1-x_n)$. The inverse map in state space I^L is given as $\boldsymbol{f}^{-1}_{\mathrm{L}s_n}(\boldsymbol{x}_n) = [1 + (2\boldsymbol{s}_n - 1)\sqrt{1-\boldsymbol{x}_n}]/2$. We obtain that

$$\begin{aligned}\boldsymbol{x}_n &= \boldsymbol{H}^{-1}_{\mathrm{L}\boldsymbol{s}_n}(\boldsymbol{x}_{n+1})\\ &= \boldsymbol{f}^{-1}_{\mathrm{L}\boldsymbol{s}_n} \circ \boldsymbol{A}^{-1}(\boldsymbol{x}_{n+1})\\ &= [1 + (2\boldsymbol{s}_n - 1)\sqrt{1 - \boldsymbol{A}^{-1}(\boldsymbol{x}_{n+1})}]/2. \quad (10)\end{aligned}$$

The CD of the inverse map $\boldsymbol{H}^{-1}_{\mathrm{L}\boldsymbol{s}_n}$ of Logistic lattice is investigated first. Define

$$\begin{aligned}&d(\boldsymbol{H}^{-1}_{\mathrm{L}\boldsymbol{s}_n}(\boldsymbol{x}_n), \boldsymbol{H}^{-1}_{\mathrm{L}\boldsymbol{s}_n}(\boldsymbol{y}_n))\\ &= d(\boldsymbol{f}^{-1}_{\mathrm{L}\boldsymbol{s}_n}(\mathbf{x}'_n), \boldsymbol{f}^{-1}_{\mathrm{L}\boldsymbol{s}_n}(\boldsymbol{y}'_n))\\ &= \max_{1\le i\le L}\left|\sqrt{1-\alpha'_n} - \sqrt{1-\beta'_n}/2\right|\\ &\le \max_{1\le i\le L}\left[1/\left(2\left|\sqrt{1-\alpha'_n} + \sqrt{1-\beta'_n}\right|\right)\right]\\ &\quad \times \left\|\boldsymbol{A}^{-1}\right\| d(\boldsymbol{x}_n, \boldsymbol{y}_n), \quad (11)\end{aligned}$$

and let $\lambda_n = \max\limits_{1\le i\le L}[1/(2|\sqrt{1-\alpha_n^i} - \sqrt{1-\beta_n^i}|)]$. It is assumed that λ_n achieves its maximum value if $i = p$. We can conclude that the inverse of Logistic map is a convergent map and $\boldsymbol{A}^{-1}$ is divergent. Moreover, $\left\|\boldsymbol{A}^{-1}\right\| \ge 1$ holds. As the value of $||\boldsymbol{A}^{-1}||$ gradually increases, $\gamma_{H^{-1}_{s_n}} = \gamma_{A^{-1}} \cdot \gamma_{f^{-1}_{s_n}}$ continuously increases. When the coupling is weak interaction, $||\boldsymbol{A}^{-1}||$ is relatively small and $\gamma_{\boldsymbol{H}^{-1}_{\mathrm{L}s_n}} < 1$ holds in the major part of the whole inverse iterations. In this case, the inverse mapping $\boldsymbol{H}^{-1}_{\mathrm{L}\boldsymbol{s}_n}$ of CML system is WC, accompanied by a little scattering behaviour. The initial conditions of the complex system can be recovered by iterating (10) infinitely. As the coupling coefficient grows bigger, the value of $\left\|\boldsymbol{A}^{-1}\right\|$ increases quickly. Consequently, there exists a case where the strength of $\gamma_{H^{-1}_{\mathrm{L}\boldsymbol{s}_n}} \ge 1$ is far more than that of $\gamma_{H^{-1}_{\mathrm{L}\boldsymbol{s}_n}} < 1$. In other words, the coupling is strong, $\boldsymbol{H}^{-1}_{\mathrm{L}\boldsymbol{s}_n}$ may be WD, and the initial conditions of the system cannot be recovered by the proposed algorithm in this contribution.

3.2.2. CD of $\boldsymbol{H}^{-1}_{\boldsymbol{T}\boldsymbol{s}_n}$

Tent map is described as $f_{\mathrm{T}}(x_n) = 1 - 2\,|x_n - 1/2|$. The corresponding inverse map in phase space I^L is defined as

$$\boldsymbol{f}_{\mathrm{T}s_n}(\boldsymbol{x}_n) = [1 + (2\boldsymbol{s}_n - 1)(1 - \boldsymbol{x}_n)]/2, \quad (12)$$

where

$$\boldsymbol{s}_n = \begin{cases} 0, & \boldsymbol{x}_n \in [0, 0.5],\\ 1, & \boldsymbol{x}_n \in (0.5, 1]. \end{cases}$$

Therefore, the inverse map of Tent-CML is given as

$$\begin{aligned}\boldsymbol{x}_n &= \boldsymbol{H}^{-1}_{\mathrm{T}s_n}(\boldsymbol{x}_{n+1})\\ &= \boldsymbol{f}^{-1}_{\mathrm{T}s_n} \circ \boldsymbol{A}^{-1}(\boldsymbol{x}_{n+1})\\ &= [1 + (2\boldsymbol{s}_n - 1)(1 - \boldsymbol{A}^{-1}(\boldsymbol{x}_{n+1}))]/2. \quad (13)\end{aligned}$$

Similarly, the CD of the inverse map $\boldsymbol{H}^{-1}_{\mathrm{T}\boldsymbol{s}_n}$ of Tent lattice can be defined as

$$\begin{aligned}&d(\boldsymbol{H}^{-1}_{\mathrm{T}s_n}(\boldsymbol{x}_n), \boldsymbol{H}^{-1}_{\mathrm{T}s_n}(\boldsymbol{y}_n))\\ &= d(\boldsymbol{f}^{-1}_{\mathrm{T}s_n}(\boldsymbol{x}'_n), \boldsymbol{f}^{-1}_{\mathrm{T}s_n}(\boldsymbol{y}'_n))\\ &= 1/2 d(\boldsymbol{x}'_n, \boldsymbol{y}'_n)\\ &\le 1/2\left\|\boldsymbol{A}^{-1}\right\| d(\boldsymbol{x}_n, \boldsymbol{y}_n), \quad (14)\end{aligned}$$

with

$$\begin{aligned}d(\boldsymbol{x}_n, \boldsymbol{y}_n) &= d(\boldsymbol{A}\boldsymbol{x}'_n, \boldsymbol{A}\boldsymbol{y}'_n)\\ &= \|\boldsymbol{A}\boldsymbol{x}'_n - \boldsymbol{A}\boldsymbol{y}'_n\|\\ &\le \|\boldsymbol{A}\|\,\|\boldsymbol{x}'_n - \boldsymbol{y}'_n\|\\ &= \|\boldsymbol{x}'_n - \boldsymbol{y}'_n\|\\ &= d(\boldsymbol{x}'_n, \boldsymbol{y}'_n). \quad (15)\end{aligned}$$

From inequalities (14) and (15), we obtain that $1/2 d(\boldsymbol{x}_n, \boldsymbol{y}_n) \le d(\boldsymbol{x}'_n, \boldsymbol{y}'_n) \le 1 \,/\, 2\left\|\boldsymbol{A}^{-1}\right\| d(\boldsymbol{x}_n, \boldsymbol{y}_n)$. Obviously, the convergent and divergent factor $k_{\boldsymbol{H}^{-1}_{\mathrm{T}\boldsymbol{s}_n}}(n)$ of $\boldsymbol{H}^{-1}_{\mathrm{T}\boldsymbol{s}_n}$ belongs to $[1/2, \left\|\boldsymbol{A}^{-1}\right\|/2]$, which is determined by $\left\|\boldsymbol{A}^{-1}\right\|$. When $\left\|\boldsymbol{A}^{-1}\right\| < 2$, we have $1/2 \le k_{\boldsymbol{H}^{-1}_{\mathrm{T}\boldsymbol{s}_n}}(n) < 1$, for any $n \in N$. Obviously, $\boldsymbol{H}^{-1}_{\mathrm{T}\boldsymbol{s}_n}$ is a contraction map. On the other hand, when $\left\|\boldsymbol{A}^{-1}\right\| \ge 2$, both convergent and divergent behaviours may exist for $\boldsymbol{H}^{-1}_{\mathrm{T}\boldsymbol{s}_n}$. That is to say, $\boldsymbol{H}^{-1}_{\mathrm{T}\boldsymbol{s}_n}$ is not a global contraction map. However, when the

convergent strength is far greater than the divergent strength, $\boldsymbol{H}^{-1}_{\mathrm{T}\boldsymbol{s}_n}$ is WC in the backward iteration process. Otherwise, $\boldsymbol{H}^{-1}_{\mathrm{T}\boldsymbol{s}_n}$ is WD, and estimating initial condition of CML is unfeasible in this case. As $\boldsymbol{H}^{-1}_{\mathrm{T}\boldsymbol{s}_n}$ is a contraction or WC map, we can recover the initial condition by using Eq. (13).

4. Analysis of error bound

If the ergodicity is preserved by the coupling, any point in the coupled chaotic system is labeled differently under the generating partition. Thus any two points on the attractors can be represented by different semi-infinite symbol sequences.[20] Meanwhile, when the number of the successive iterations increases, the $\bigcap_{n=0}^{N-1} H^{-n}P_{s_n}$ will provide us more accurate information about $\boldsymbol{x}_0$. The average rate of information production is given by the metric entropy h for the generating partitions. Assuming that the error of estimation is uniformly distributed on $\bigcap_{n=0}^{N-1} H^{-n}P_{s_n}$, correspondingly, it can be written as

$$-\frac{1}{N}\sum_{n=0}^{N-1}\ln\left|\frac{\bigcap_{i=0}^{n-1} H^{-i}P_{\boldsymbol{s}_i}}{\bigcap_{i=0}^{n} H^{-i}P_{\boldsymbol{s}_i}}\right| \approx h, \tag{16}$$

where $|.|$ represents the size of a set. Therefore, the estimated error can be bounded by

$$\text{error} = \sum_{i=1}^{N}(\hat{x}_n^i - x_n^i)^2 \leq \left|\bigcap_{i=0}^{N-1} H^{-i}P_{\boldsymbol{s}_i}\right| \approx \sqrt{D}\,\mathrm{e}^{-hN/2}, \tag{17}$$

where the constant D is the attractor size. It can be seen from Eq. (17) that the proposed method converges exponentially fast in the noise-free case. h is also called KS-entropy density, which is equal to the average of the sum of all the positive Lyapunov exponents. It can be described as[21]

$$h = \frac{1}{L}\sum_{\lambda_i>0}\lambda_i, \tag{18}$$

where $(\lambda_1, \lambda_2, \ldots, \lambda_L)$ is the corresponding Lyapunov spectrum for the CML system, which is defined as

$$\lambda_i = \ln\beta + \ln[1-\varepsilon+\varepsilon\cos(2\pi i/L)], (i = 1, 2, \ldots, L), \tag{19}$$

where $\ln\beta$ denotes the Lyapunov exponent of local dynamics function in CML. For unimodal chaotic Logistic map and Tent map, their Lyapunov exponents are both equal to $\ln 2$. Therefore, when the system parameters (i.e. ε and L) are the same for Logistic-CML and Tent-CML, they have the same Lyapunov spectrum. Furthermore, their metric entropy h according to Eq. (18) and the dimension D of attractors defined as Eq. (20) are the same.[21]

$$D = \begin{cases} 0, & \text{if there is no such } k, \\ k + \dfrac{1}{|\lambda_{k+1}|}\sum\limits_{i=1}^{k}\lambda_i, & \text{if } k < L, \\ L, & \text{if } k = L, \end{cases} \tag{20}$$

where k is the largest integer such that $\sum_{i=1}^{k}\lambda_i \geq 0$. The Lyapunov dimension furnishes an estimation of the information dimension of the attractor embedded in the L-dimensional phase space of the CML system, which is the dimension associated with the most representative part of its nature measure. Hence, D provides an important indicator for measuring the complexity of the phase space of such a spatiotemporal chaotic system.[21]

Figure 2 shows the relationship between metric entropy and coupling strength under different values of system size. It can be seen that the system size basically has little effect on KS-entropy density when the coupling intensities of CML systems are the same because KS-entropy density is the average of the sum of the positive Lyapunov exponents and augments with the increase of the total positive exponent. When the coupling strength becomes stronger, the local reaction of the system decreases whereas the spatial diffusion reinforces, which leads to the decrease of the intensity contrast between the spatiotemporal chaos and the site diffusibility. In this case, more positive exponents become small rapidly, and the KS-entropy density therefore declines with the increase of the space coupling, as shown in the case of $\varepsilon \leq 0.25$ in Fig. 2. When the coupling strength continues to increase, i.e., for the case of $0.25 < \varepsilon \leq 0.5$, the KS-entropy density gradually decreases.

Figure 3 displays the relationship between the dimension of attractors D and coupling strength ε under different values of system size L, which indicates that the dimension of attractor is directly related with the number of the sites in CML. For $\varepsilon \in [0, 0.4]$, we have $\lambda_1 + \lambda_2 + \cdots + \lambda_L > 0$ and the dimension of attractor is equal to the system size. When $0.4 < \varepsilon \leq 0.5$, some positive Lyapunov exponents turn into negative values, which leads to $\lambda_1 + \lambda_2 + \cdots + \lambda_L < 0$. So there exists such a maximum integer k that $\sum_{i=1}^{k}\lambda_i > 0$ and $\sum_{i=1}^{k+1}\lambda_i < 0$. In this case, we have the dimension of attractor $D = k + (\sum_{i=1}^{k}\lambda_i)/|\lambda_{k+1}|$. Furthermore, with the increase of the number of sites, k will change

faster and the value of D goes down faster correspondingly as shown in Fig. 3.

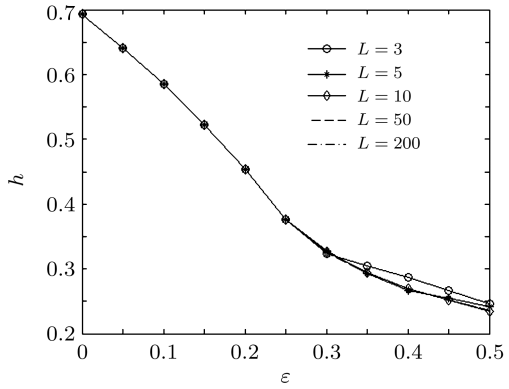


Fig. 2. Relationships between KS-entropy density h and coupling strength ε under different values of system size L.

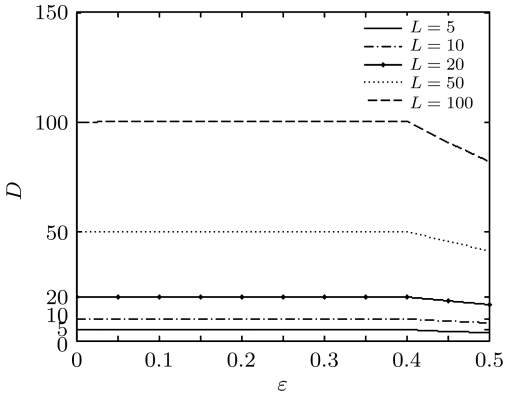


Fig. 3. Relationships between dimension of attractor D and coupling strength ε under different values of system size L.

5. Performance characteristics

All the initial values are randomly selected from [0,1]. We continually iterate Eq. (4) according to the chosen initial condition, and obtain the symbol s_n^i and state value x_n^i in the ith site of the CML system. According to $\boldsymbol{x}_n = \boldsymbol{H}_{\boldsymbol{s}_n}^{-1}(\boldsymbol{x}_{n+1})$ with respect to symbolic sequence length increasing, the estimated value $\hat{x}_n^i$ of each site can be obtained at each iteration. The variance of the estimator for $\boldsymbol{x}(0)$ can be calculated as

$$\lg(\text{error}) = \lg\left(\sum_{i=1}^{L}\left(x_n^i - \hat{x}_n^i\right)^2\right). \tag{21}$$

The convergent rates of the algorithm for Logistic-CML and Tent-CML are depicted in Fig. 4(a) and 4(b) respectively. The total number of sites is $L = 20$, and the total iteration length is $N = 20$. These two figures show that the weaker the coupling strength ε is, the better the whole convergent performance for the estimator is and the faster the convergence is. The divergent strength becomes stronger when the coupling coefficient continuously increases. Meanwhile, the global convergent performance becomes worse and the convergent rate gradually diminishes. This is consistent with the theoretic analysis given above. The performance of the estimator is related not only to the symbolic sequence length, but also to the comparable strength between the convergence and the divergence. When the inverse system is globally contracting or WC, the initial condition of CML can be recovered with respect to sufficient backward iteration.

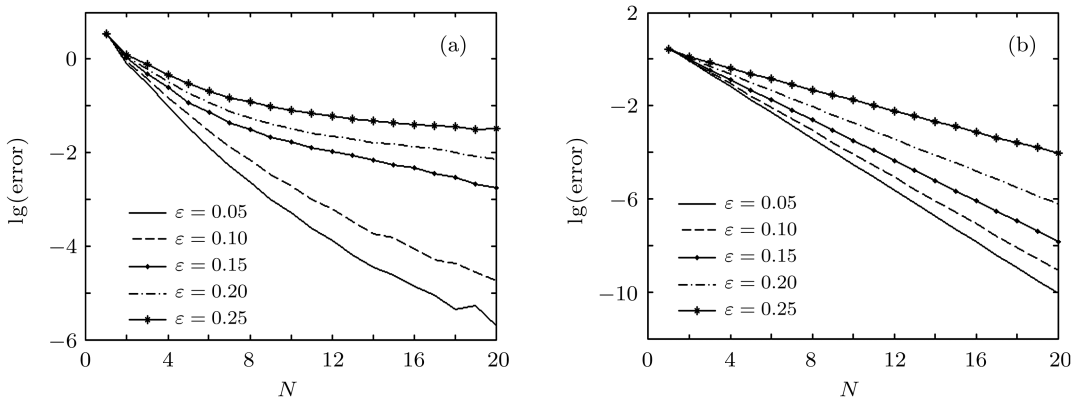


Fig. 4. Convergent performances of (a) Logistic-CML and (b) Tent-CML.

By comparing Fig. 4(a) with Fig. 4(b), it can be found that the error of the Logistic-CML estimator is greater than that of Tent-CML estimator under the same iterations when the system parameters (i.e., L and ε) of Logistic-CML and Tent-CML are the same. Meanwhile, the global convergent performance of the former is

better than that of the latter. This is because when the coupling coefficient is no longer more than 0.25 and the system size is 20, Fig. 1(b) indicates that $\left\|\boldsymbol{A}^{-1}\right\| < 2$, the inverse map of Logistic-CML is globally contracting, yet that of Tent-CML is WC. In addition, it can be seen from Figs.4 and 5 that the error is always less than the error bound (i.e., $\sqrt{D}\,\mathrm{e}^{-hN/2}$) in each iteration, and gradually tends to zero as the symbolic sequence length increases.

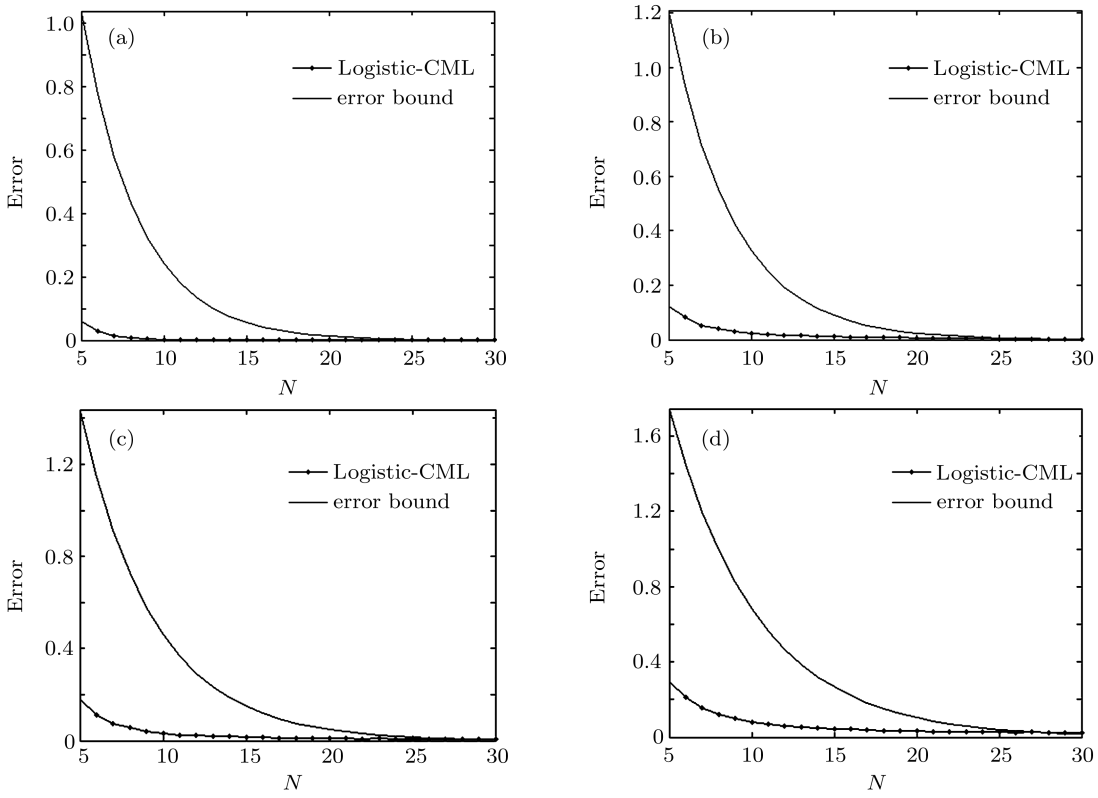


Fig. 5. Values of error bound ($\sqrt{D}\,\mathrm{e}^{-hN/2}$) in backward iteration process for different values of coupling strength ε: $\varepsilon = 0.10$ (a), 0.15 (b), 0.20 (c), and 0.25 (d).

6. Conclusion

The convergence for the inverse problem of CML system is investigated in this paper. It is found that the convergence is related not only to the coupling strength, but also to the selected dynamic mapping function. The strength contrast between the two factors determines the CD of global iteration process. The coupling coefficient plays a key role in the CD. When the inverse map of CML system is not a contracting map or it is undeterminable, WC and WD are taken as a foundation to determine whether the initial conditions can be recovered. Simulation results show that the initial condition of CML systems can be estimated with making sufficient backward iterations when the coupling strength is not very strong. Moreover, the error of the estimator in noiseless environment is less than $\sqrt{D}\,\mathrm{e}^{-hN/2}$ which is determined by the dimension of attractors and metric entropy of CML system. The feasibilities of the initial condition estimation in different CML systems and the error bound in each backward iteration are analysed. It is noticeable that the error caused by noise is not taken into account, however, the noise always exists actually. Therefore, it will be the key point in the next study that the initial condition of CML is estimated in noise cases. In summary, the feasibilities of the initial condition estimation in different CML systems and the error bounds in different time steps are investigated in noiseless environment. The proposed approach provides important results for better understanding the practical spatiotemporal chaotic system.

References

[1] Zhang J S 2007 *Chin. Phys.* **16** 352

[2] Chen F X and Zhang W D 2007 *Chin. Phys.* **16** 937

[3] Wang Y C, Zhao Q C and Wang A B 2008 *Chin. Phys.* B **17** 2373

[4] Sheng L Y and Jia W Y 2005 *Acta Phys. Sin.* **54** 5574 (in Chinese)

[5] Shen M F, Lin L X, Chen J L and Chang C Q 2010 *IEEE Trans on Instrum. Meas* **59** 1485

[6] Wang W H, He Y X, Gao Z, Zeng L, Zhang G P, Xie L F and Feng C H 2004 *Chin. Phys.* **13** 2091

[7] Yang W M 1994 *Spatiotemporal Chaos and Coupled Map Lattice*(Shanghai: Shanghai Scientific and Technological Education Publishing House) (in Chinese) p12

[8] Zheng W M and Hao B L 1994 *Applied Symbolic Dynamics*(Shanghai: Shanghai Scientific and Technological Education Publishing House) (in Chinese) p50

[9] Fu Z J, Zeng Y C and Xu M L 2008 *Acta Phys. Sin.* **57** 4014 (in Chinese)

[10] Xiao F H, Yan G R and Han Y H 2004 *Acta Phys. Sin.* **53** 2876 (in Chinese)

[11] Falcioni M, Palatella L, Pigolotti S and Vulpiani A 2005 *Phys. Rev.* E **72** 016220

[12] Buminovich L A 1997 *Physica* D: *Nonlinear Phenomena* **103** 1

[13] Ling C, Wu X F and Sun S G 1999 *IEEE Trans. on Signal Processing* **47** 1424

[14] Zeng Y C and Tong Q Y 2003 *Acta Phys. Sin.* **52** 285 (in Chinese)

[15] Shen M F, Liu Y and Lin L X 2009 *Chin. Phys.* B **18** 1761

[16] Wang K, Pei W J, Xia H S and He Z Y 2007 *Acta Phys. Sin.* **56** 3766 (in Chinese)

[17] Wang K, Pei W J, He Z Y and Cheung Y M 2007 *Phys. Lett.* A **367** 316

[18] Wang K, Pei W J, Wang S P, Cheung Y M and He Z Y 2008 *IEEE Trans. Ciruits Syst.* I **55** 1116

[19] Shen M F, Lin L X, Li X Y and Chang C Q 2009 *Acta Phys. Sin.* **58** 2921 (in Chinese)

[20] Shawn D P, Ned J C and Erik B 2006 *Phys. Rev. Lett.* **96** 034105

[21] Santos A M, Woellner C F, Lopes S R, Batista A M and Viana R L 2007 *Chao, Solitons and Fractals* **32** 702